

Figure S2-1:

a. Oxygen isotope ratio measurements, collected from conodont apatite, from Sun et al. (2012) and Trotter et al. (2015).

b. Number of occurrences in each substage.

c. Collection and formation counts in the Paleobiology Database; note log scale.

d. Squares diversity for terrestrial (green) and marine (blue) tetrapods.

e. Interpolated diversity through time for terrestrial tetrapods. Missing points indicate an estimated diversity of more than three times the observed value. Error bars indicate 95% confidence intervals.

f. Interpolated diversity through time for marine tetrapods. Missing points indicate an estimated diversity of more than three times the observed value. Error bars indicate 95% confidence intervals.

Stages included in time interval are Wuchiapingian, Changhsingian, Induan, Olenekian, Anisian, Ladinian and Carnian, with grey bars indicating alternate stages. The Triassic stages can be split into the Griesbachian, Dienerian, Smithian, Spathian, AegEAN, Bithynian,

Pelsonian, Illyrian, Fassanian, Longobardian, Julian and Tuvalian substages. Due to their comparatively short durations, the Induan was considered as a single time bin (Griesbachian + Dienerian), and the Anisian substages were paired (Aegean + Bithynian, and Pelsonian + Illyrian).

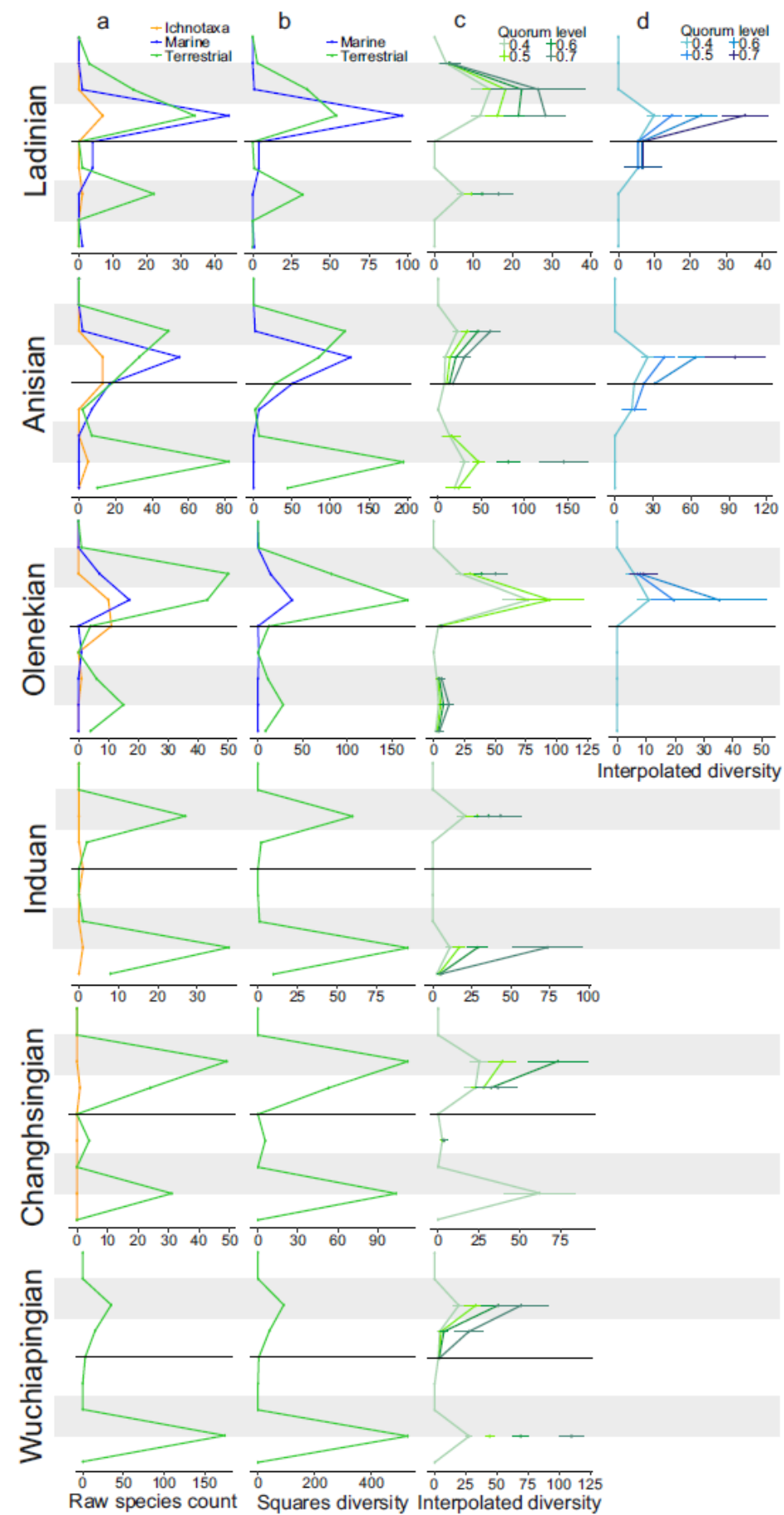


Figure S2–2: Tetrapod diversity by latitude, as in Figure 2-1, but with occurrences split into stages. Grey bars indicate 30-60°N and S.

- a. Raw occurrences within 20° latitude bins (e.g. central bin is 10°N-10°S).**
- b. Squares diversity by latitudinal bin for terrestrial (green) and marine (blue) tetrapods.**
- c. Interpolated diversity by latitudinal bin for terrestrial tetrapods. Bins with < 3 species have been plotted as '0', while missing points indicate an estimated diversity of more than three times the observed value. Error bars indicate 95% confidence intervals.**
- d. Interpolated diversity by latitudinal bin for marine tetrapods. Bins with < 3 species have been plotted as '0', while missing points indicate an estimated diversity of more than three times the observed value. Error bars indicate 95% confidence intervals. The oldest marine tetrapod fossils are Olenekian (late Early Triassic; 251-247Ma) in age.**

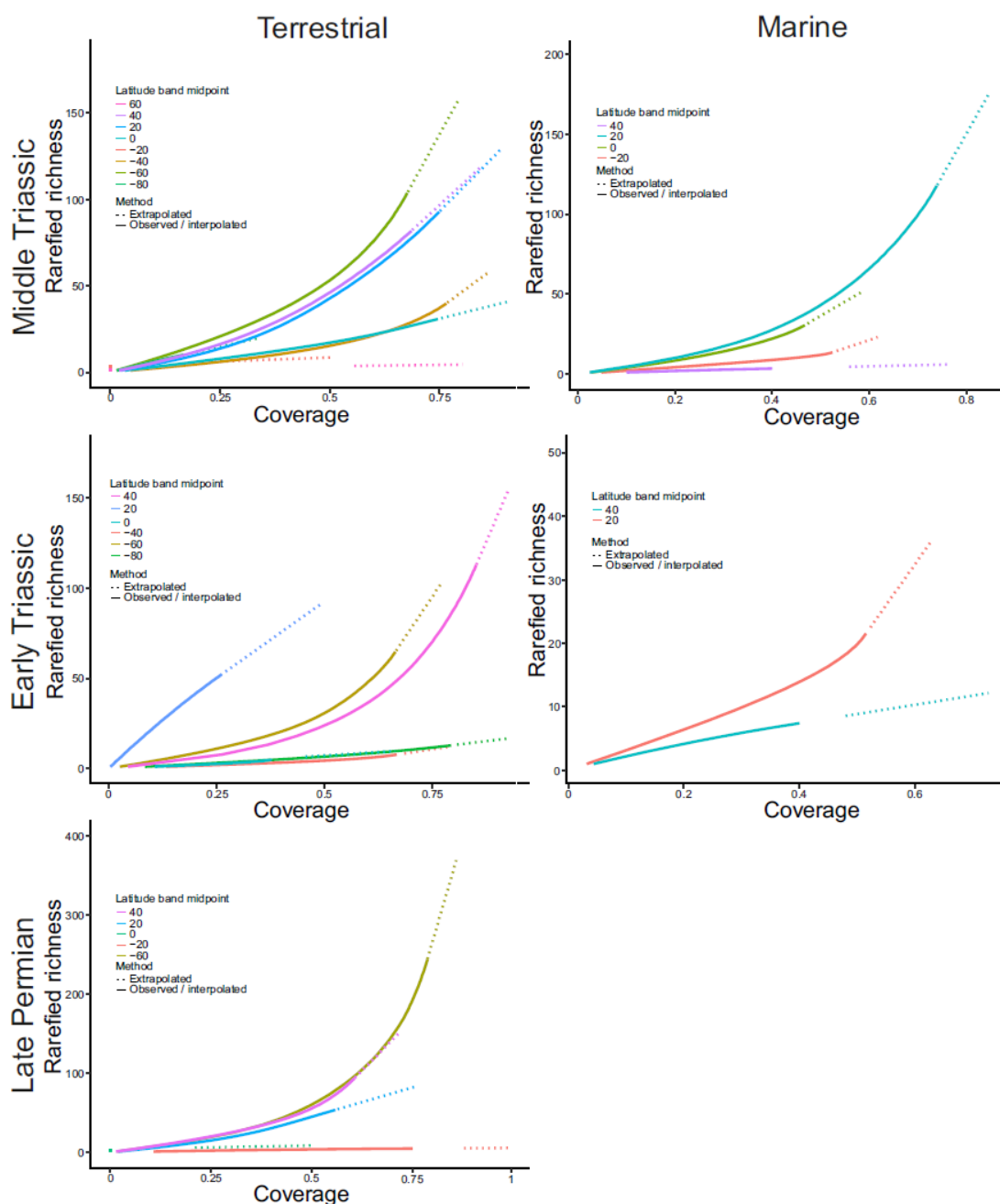


Figure S2-3: Rarefaction curves for each of the interpolation analyses in Figure 2-1, indicating the relationship between richness and sampling intensity for each bin.

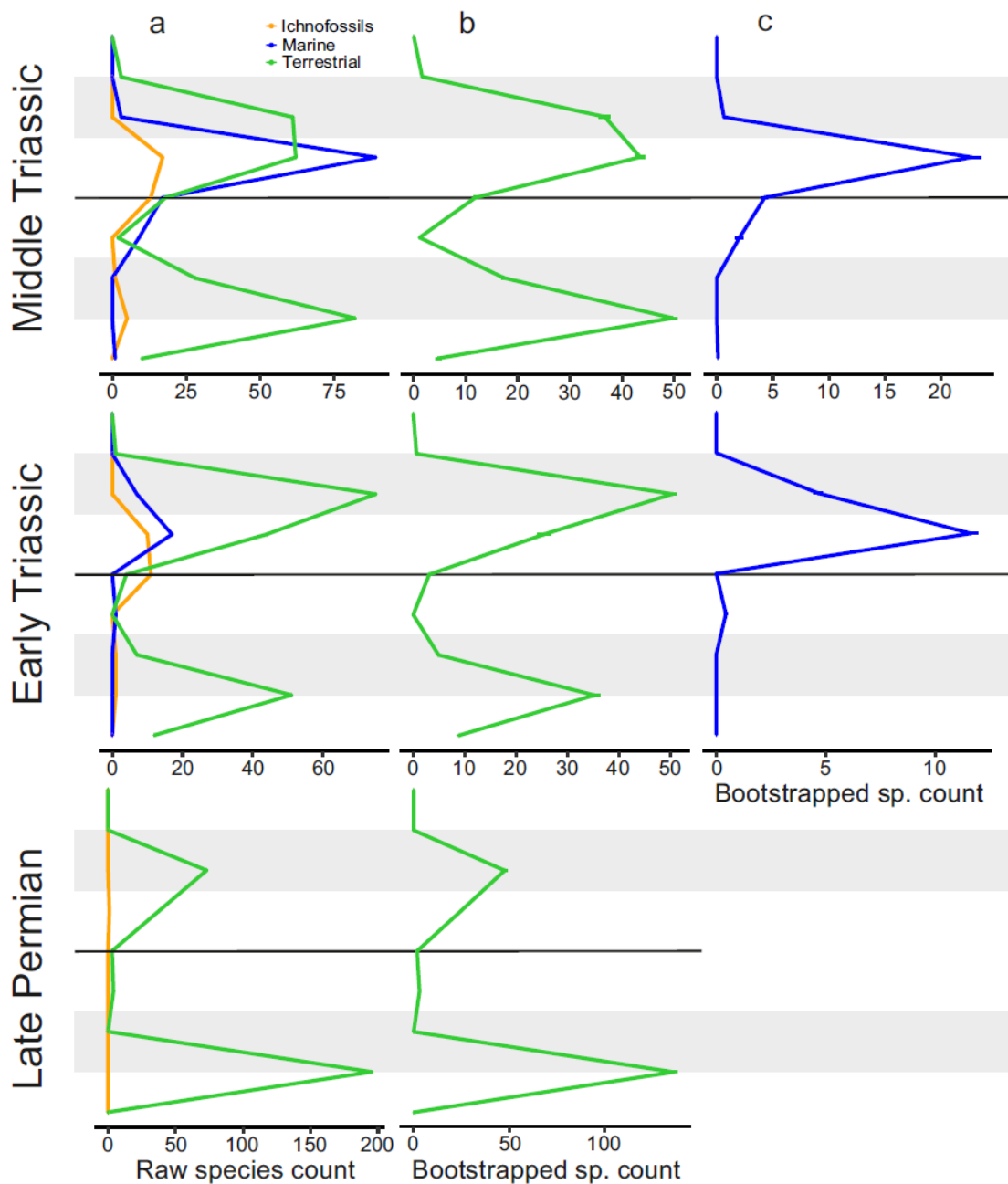


Figure S2-4: Raw species richness (a) compared with the mean of 100 bootstrap replicates of collection subsamples. The grey bars indicate 30-60°N and S. The terrestrial (b) analysis subsampled 250 collections, while the marine (c) analysis subsampled 30 collections. Error bars indicate 95% confidence intervals across the 100 replicates.

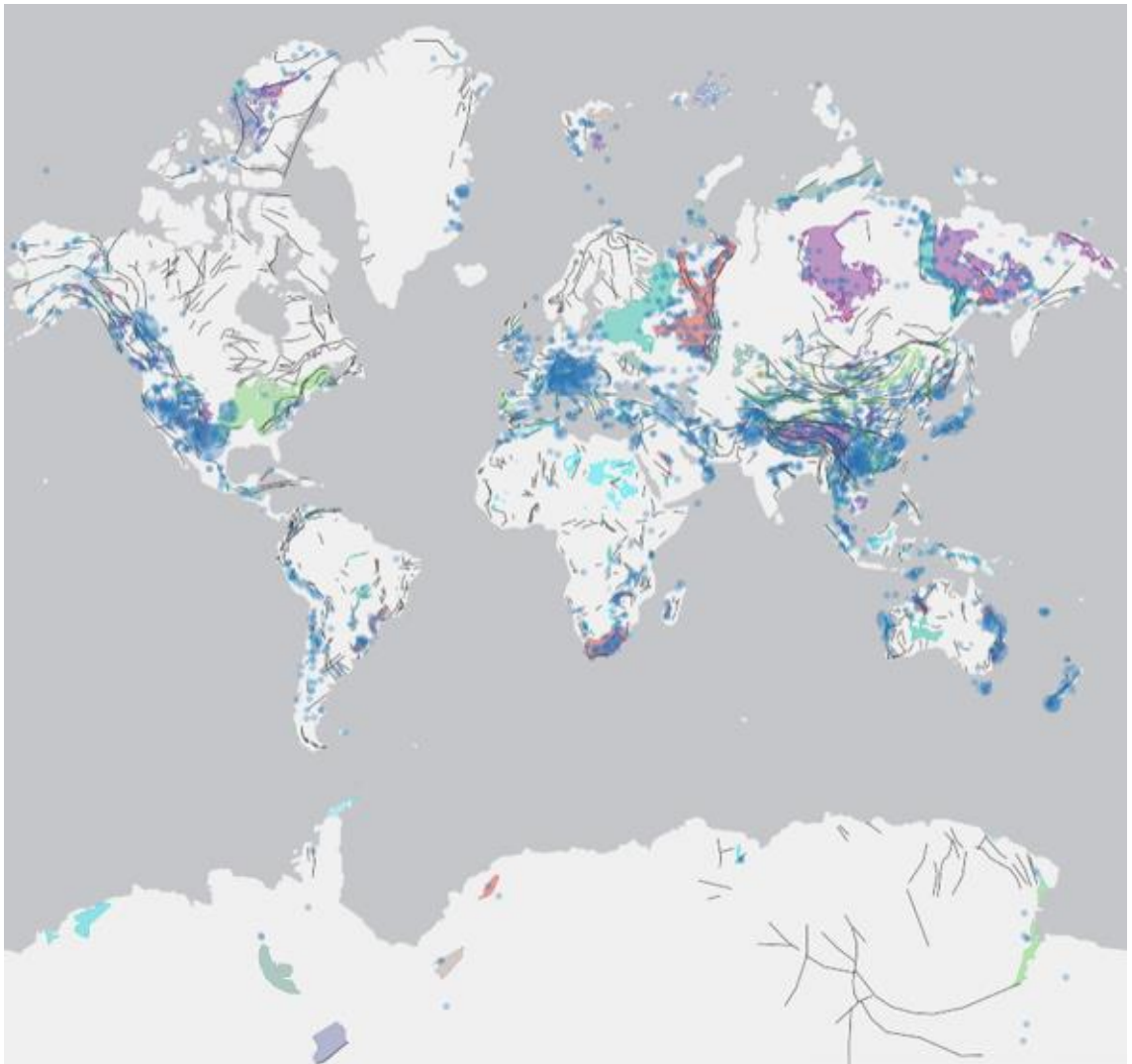


Figure S2–5: Screenshot taken from Macrostrat Map app, with Permian and Triassic rocks indicated in coloured patches, while blue dots indicate the localities of collections in the Paleobiology Database of the same age (<https://macrostrat.org/map/#/z=1.5/x=16/y=23/bedrock/fossils/intervals=75/intervals=63>).

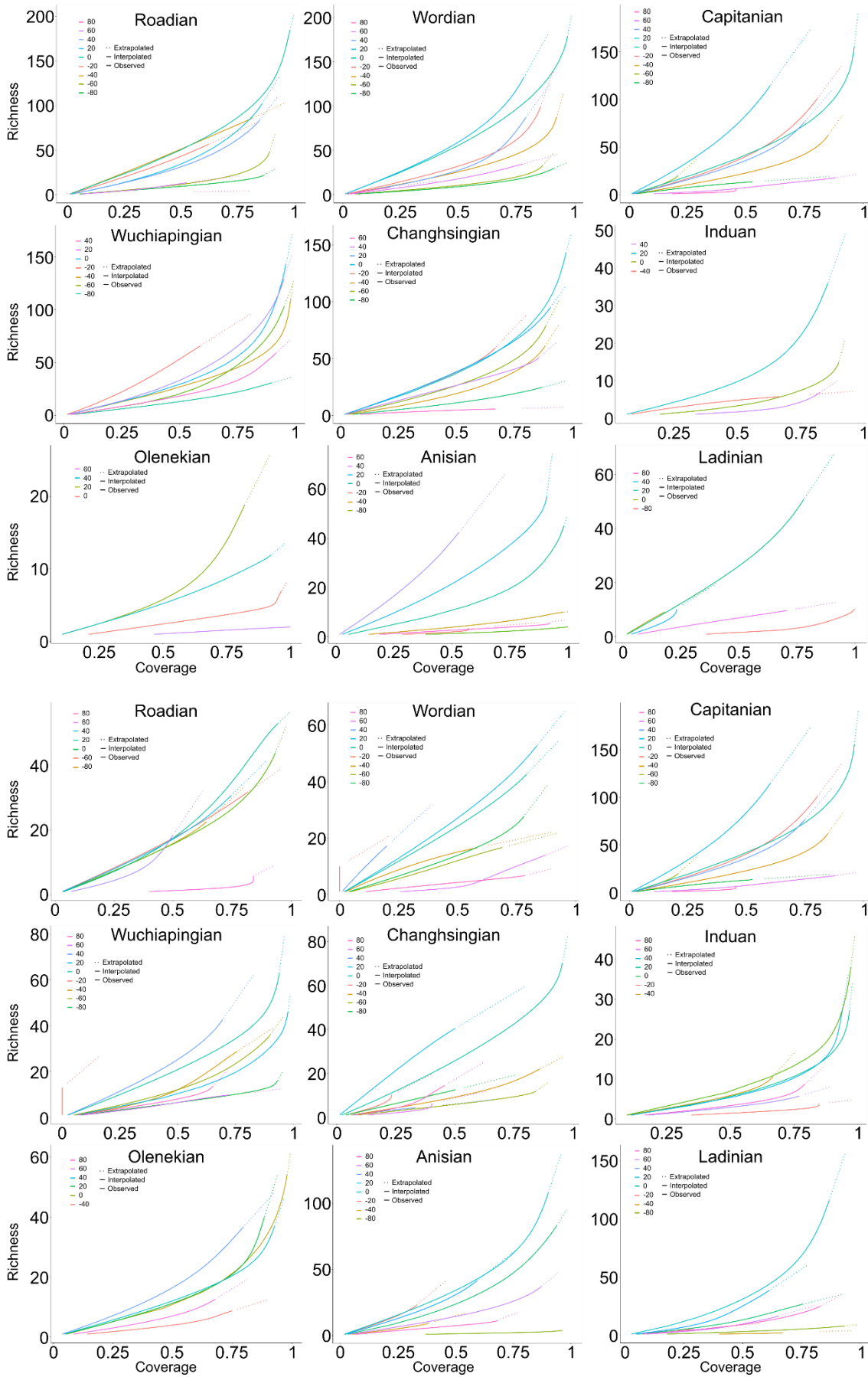


Figure S3–1: Rarefaction curves for brachiopods (top) and bivalves (bottom), relating to each of the interpolation analyses in Figure 3-2, indicating the relationship between richness and sampling intensity for each bin.

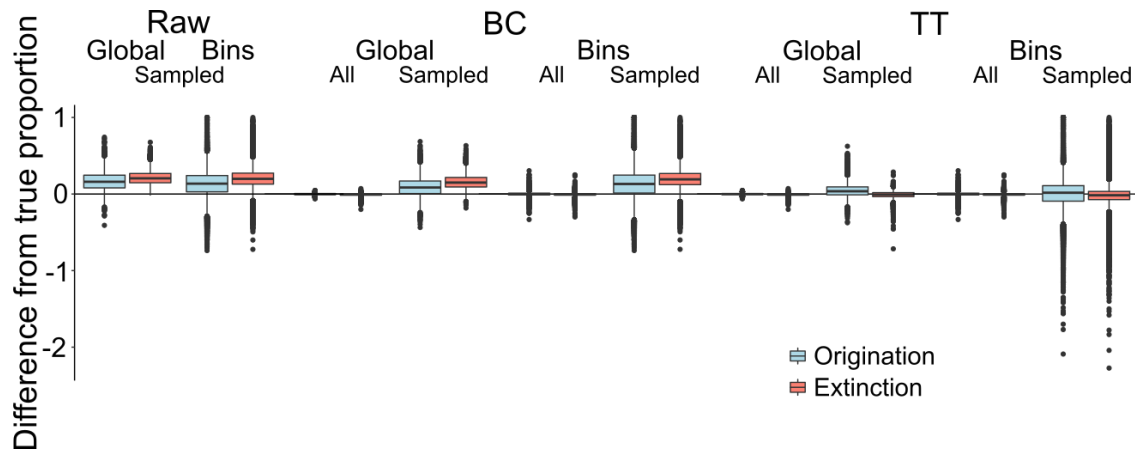


Figure S4-1: Differences between “true” and estimated proportions of origination and extinction, comparing proportions calculated at global and individual spatial bin scales produced in the main simulation (Figure 4-3).

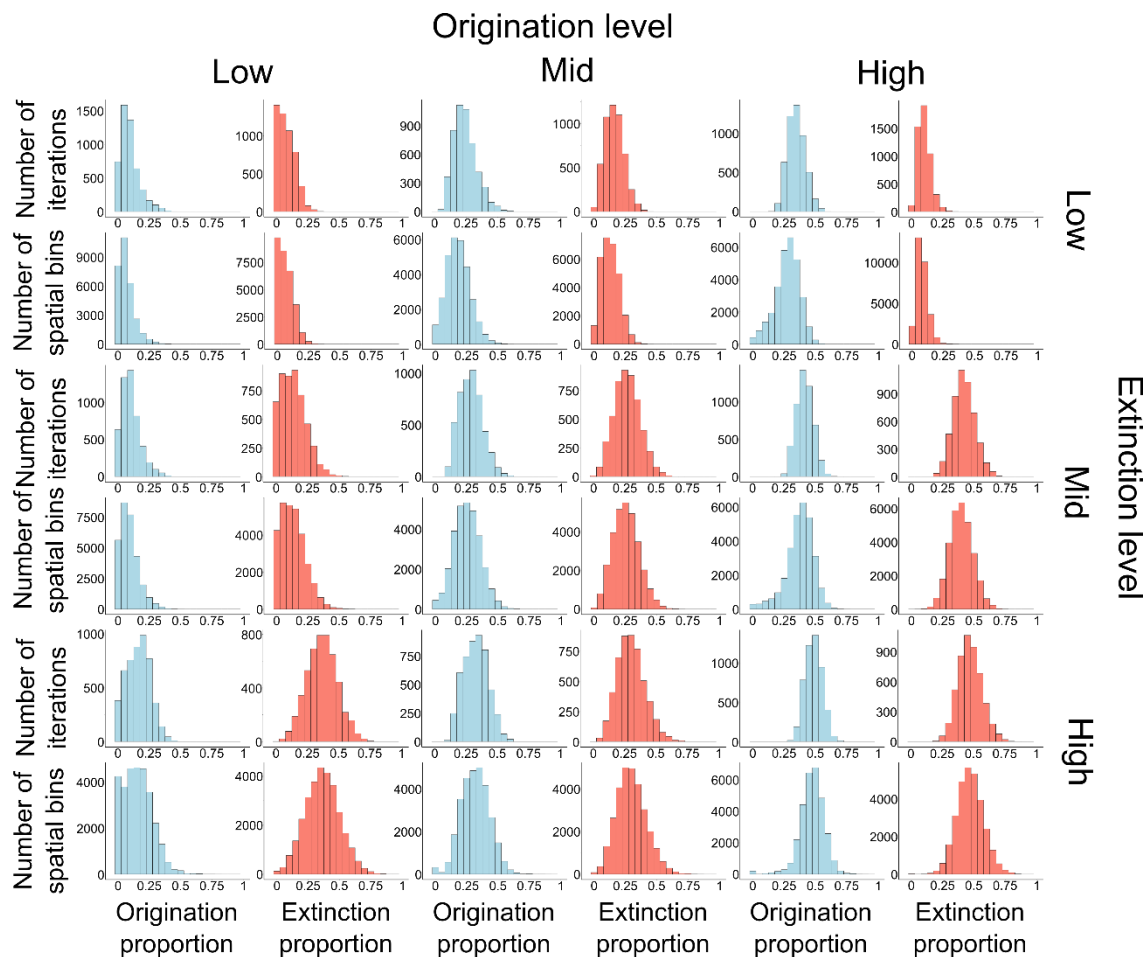


Figure S4-2: Distribution of “true” origination and extinction proportions generated within the additional simulated datasets, globally (top; 5000 iterations) and for individual spatial bins (bottom; 6 x 5000 = 30000 bins).

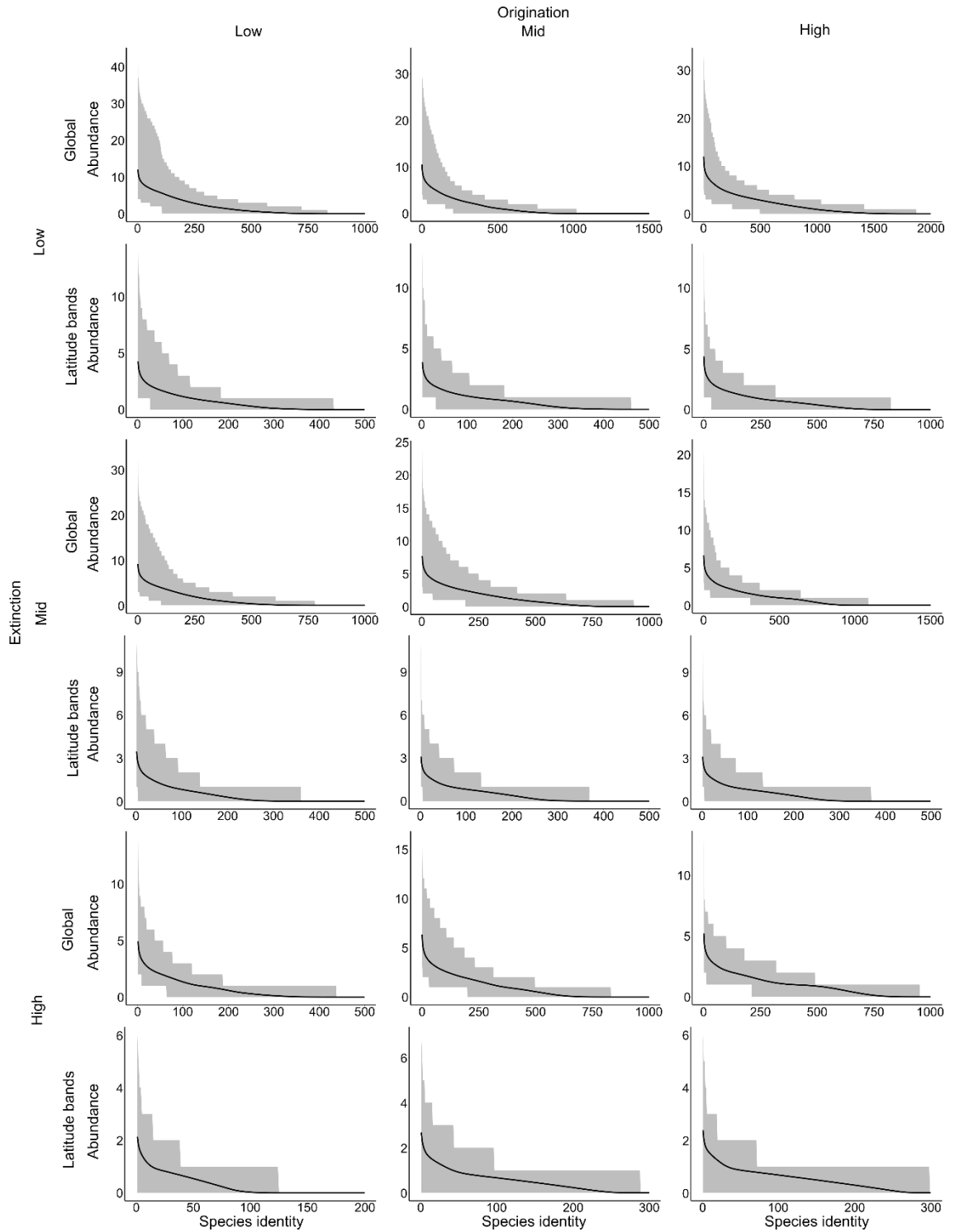


Figure S4–3: Species abundance distributions for t_1 and t_2 (the time bins for which origination and extinction were calculated) in the additional simulations, globally (top; $2 \times 5000 = 10000$ spatio-temporal bins) and for individual spatial bins (bottom; $2 \times 6 \times 5000 = 60000$ spatio-temporal bins). The black line is the mean abundance of the species found at the given identity rank, with the grey error bars showing the maximum and minimum abundance at that rank.

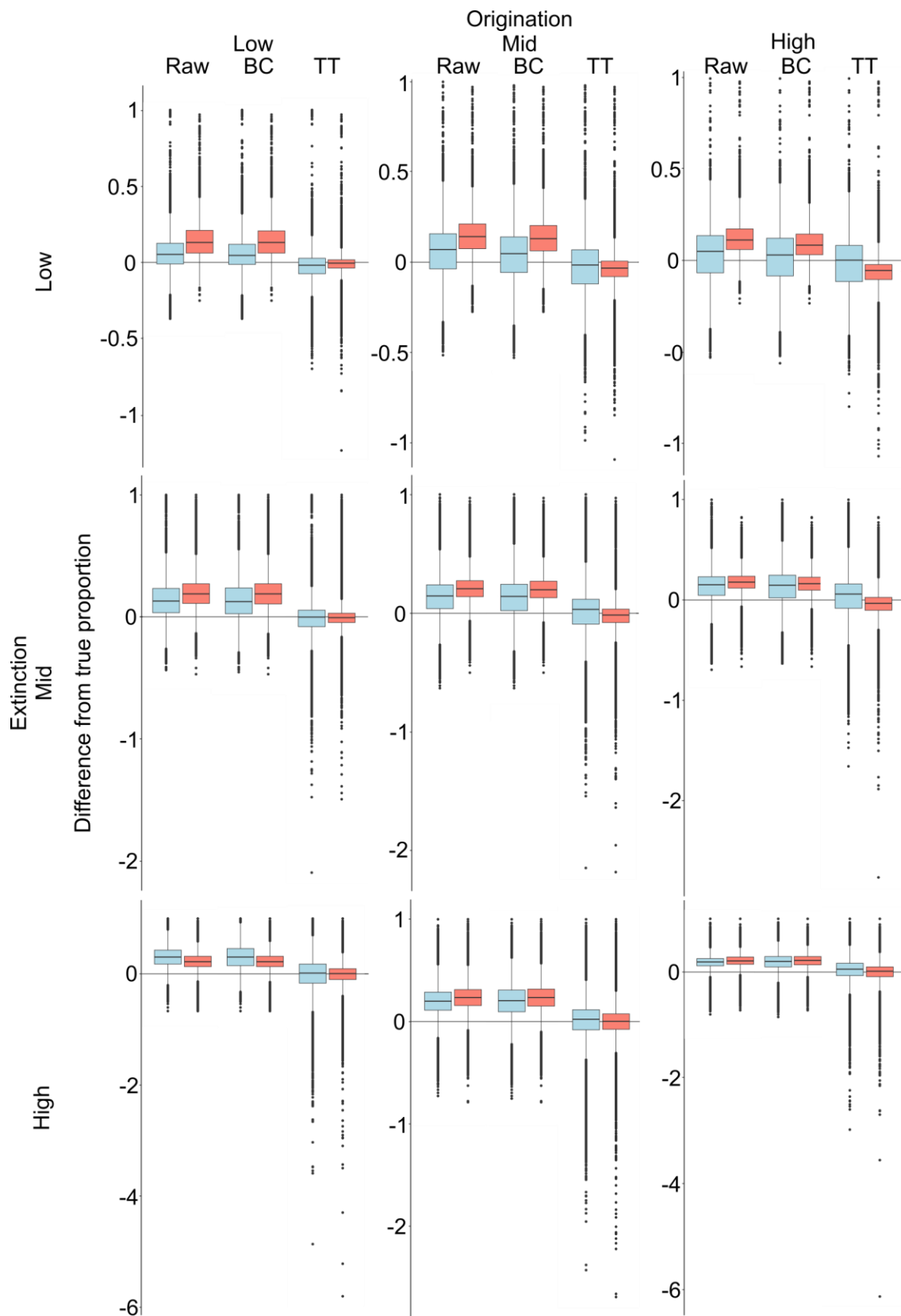


Figure S4-4: Difference between “true” and estimated proportions of origination and extinction, following sampling, across all spatial bins (n = 30000) produced in the additional simulations.

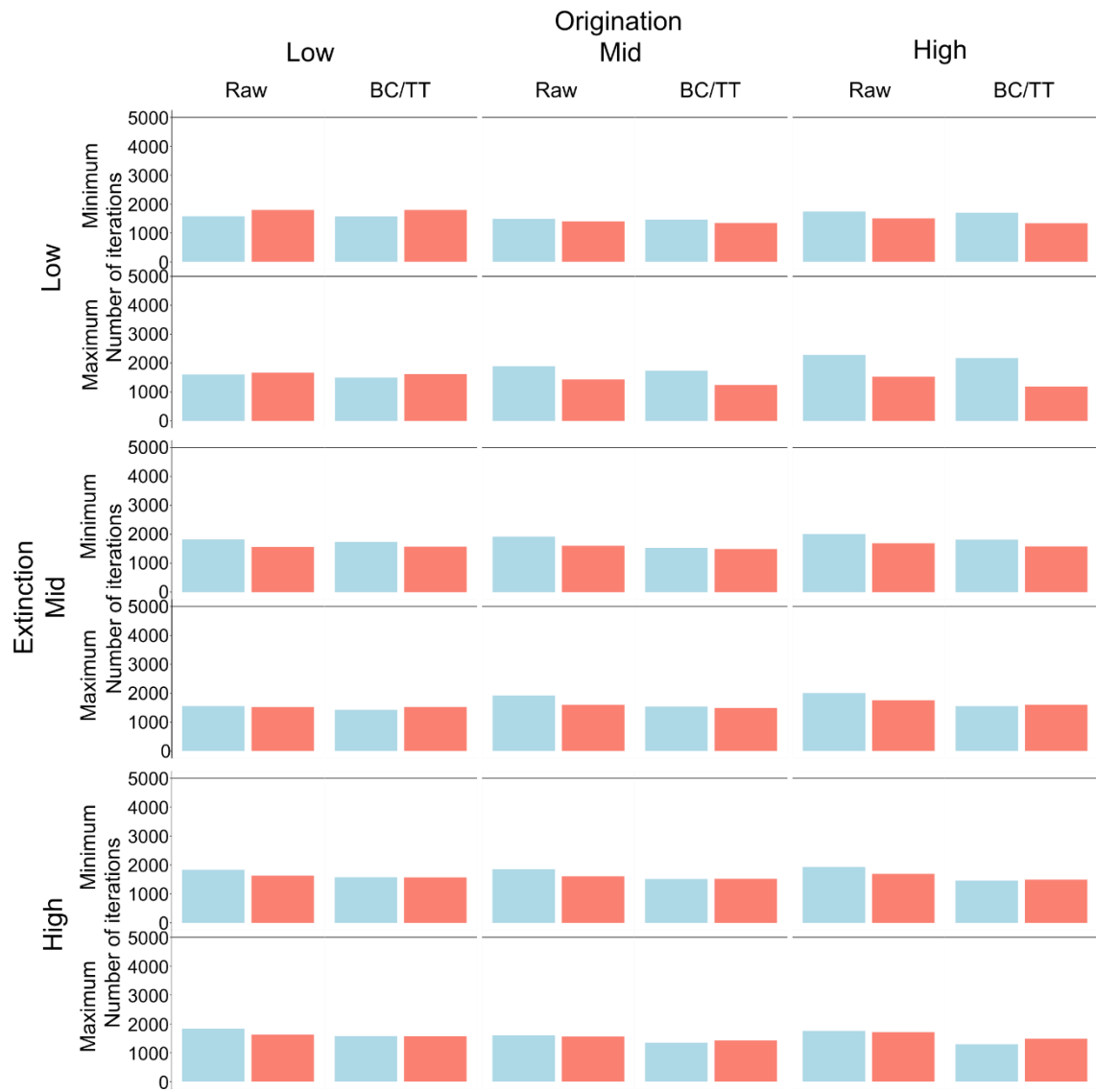


Figure S4–5: Number of iterations for which the identity of the bin with minimum and maximum proportion is preserved following sampling in the additional simulations. Boundary-crosser and three-timer methods produced identical results.

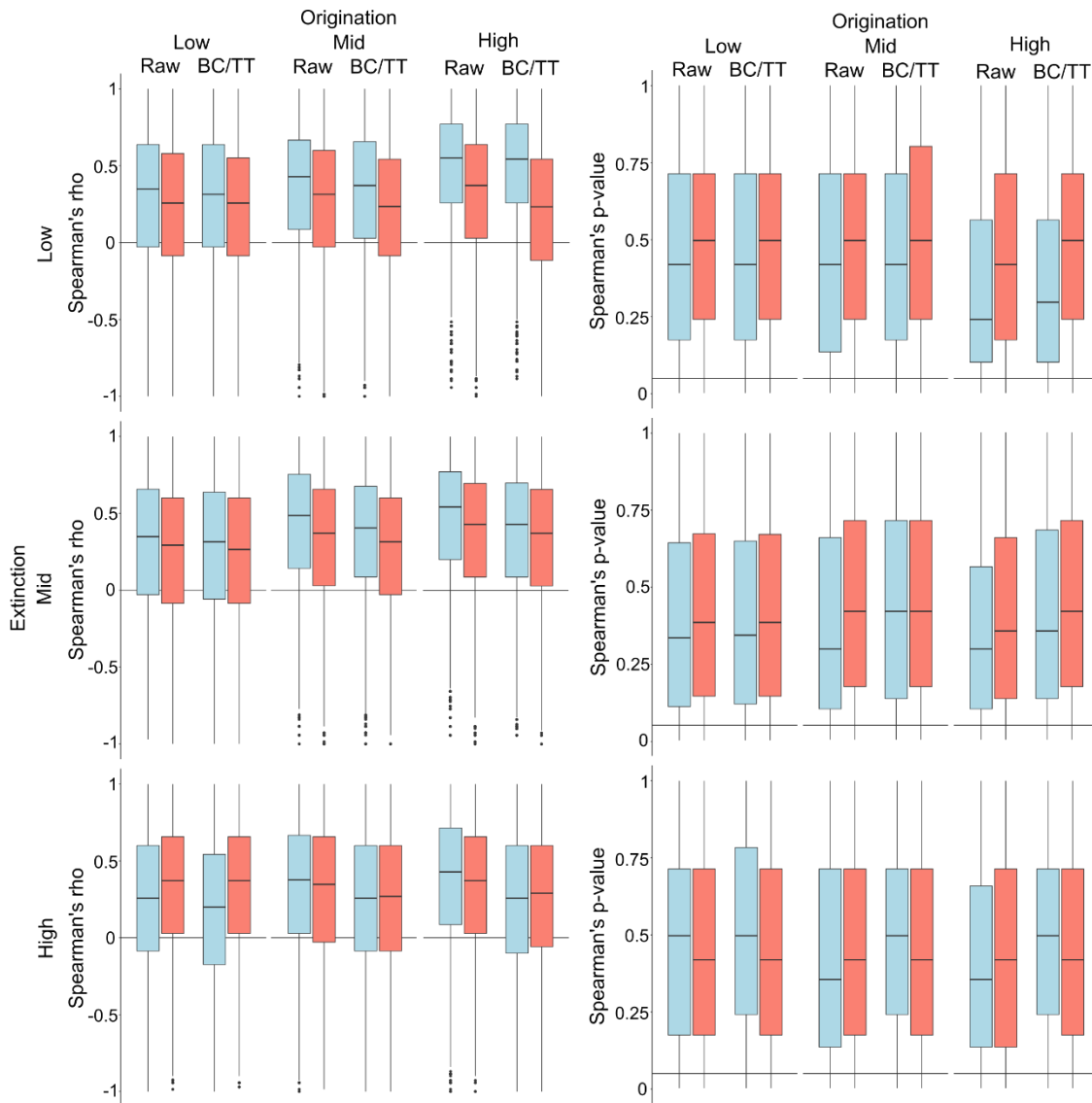


Figure S4–6: Distribution of correlation coefficients and p-values across additional simulation iterations, when comparing “true” proportions of extinction and origination to those produced post-sampling and estimation. Tests examined rank correlation using Spearman’s ρ . Boundary-crosser and three-timer methods produced identical results.

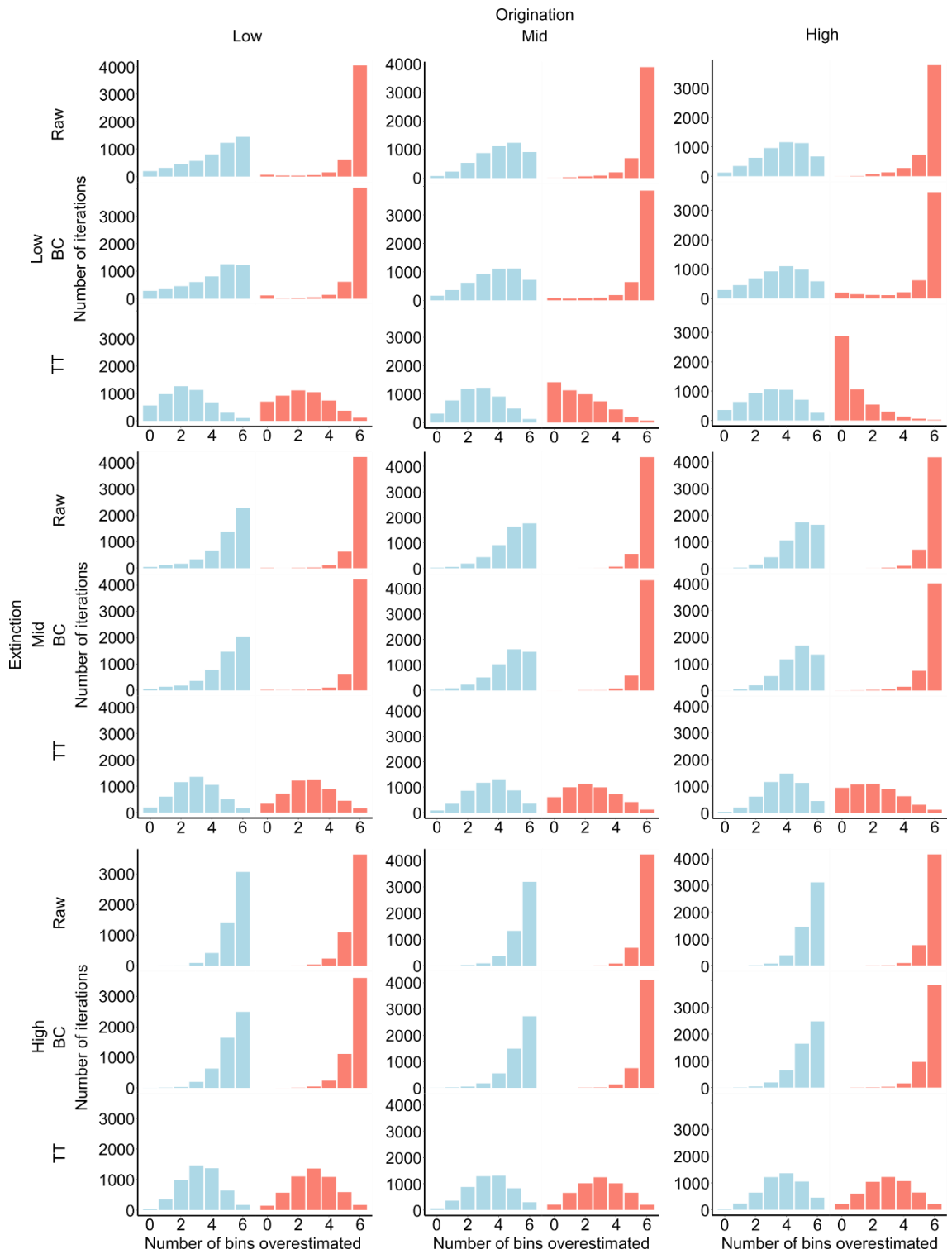


Figure S4–7: Distribution of number of spatial bins for which proportions of origination and extinction were overestimated compared to their “true” value within a given iteration in the additional simulations; for example, a value of six would mean that all bins in the iteration were overestimated, whereas a value of zero would mean that all bins in the iteration were either estimated correctly or underestimated.

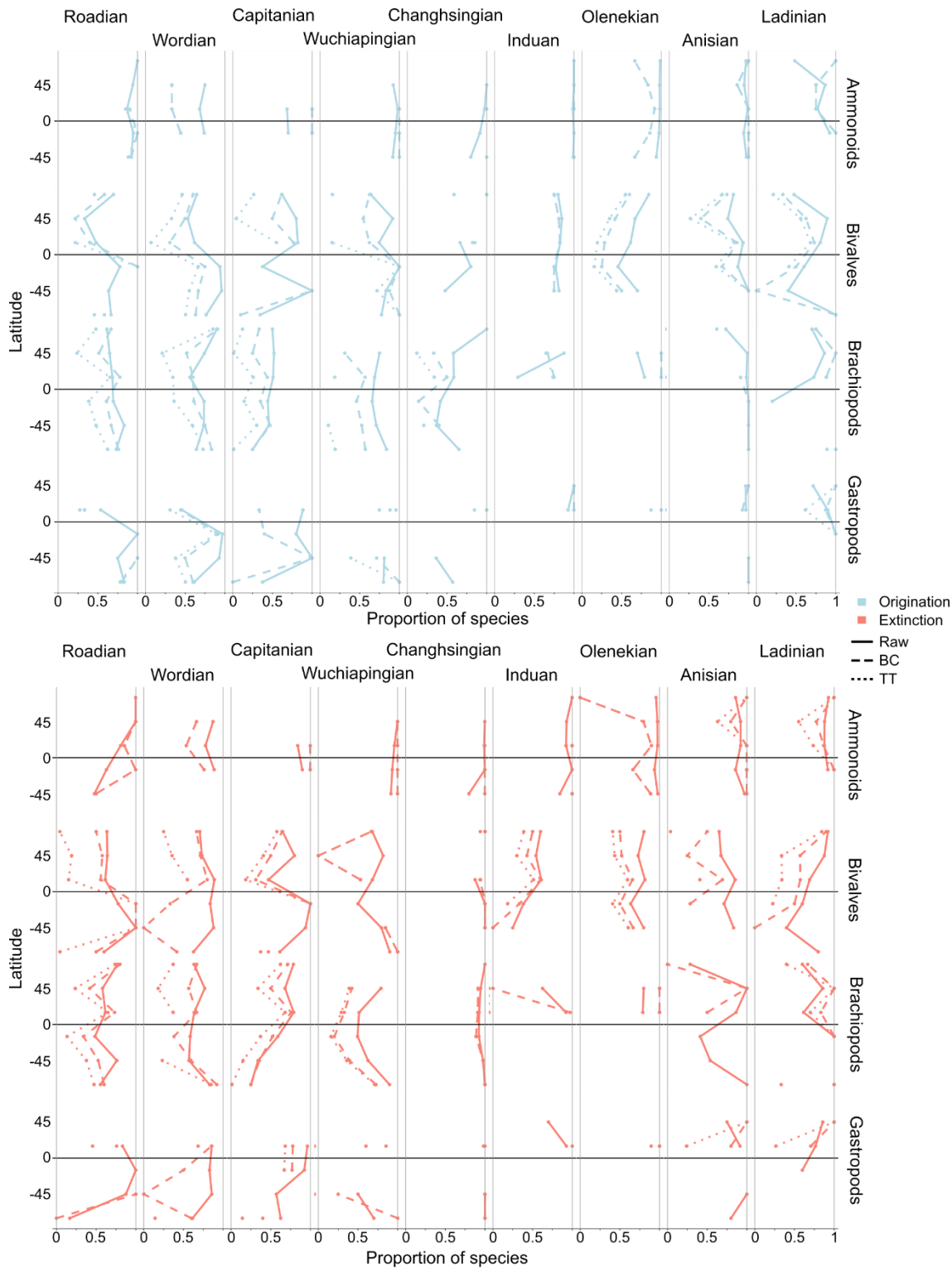


Figure S4-8: Species origination and extinction by latitude of four different marine clades in each stage of the middle Permian to Middle Triassic. Occurrences were split into six 30° latitude bins. Estimates were calculated for each spatio-temporal bin containing five or more species. Missing points indicate insufficient occurrences to calculate a proportion.